63-1-6

RADC-TDR-62-510

HIGH POWER R-F WINDOW STUDY PROGRAM

QUARTERLY TECHNICAL NOTE NO. 1

6 July Through 30 September 1962

VARIAN ASSOCIATES

PALO ALTO, CALIFORNIA

CONTRACT NO. AF 30(602)-2844

Prepared For

ROME AIR DEVELOPMENT CENTER

AIR FORCE SYSTEMS COMMAND

UNITED STATES AIR FORCE

GRIFFISS AIR FORCE BASE

NEW YORK

VARIAN REPORT NO. 304-1Q

OCTOBER 1962

RADC-TDR-62-510

HIGH POWER R-F WINDOW STUDY PROGRAM

Quarterly Technical Note No. 1
6 July Through 30 September 1962

VARIAN ASSOCIATES

Palo Alto, California

Contract No. AF 30(602)-2844
Project No. 5573
Task No. 557303

Prepared by: Floyd Johnson
Approved by: L. T. Zitelli

Prepared for

ROME AIR DEVELOPMENT CENTER
AIR FORCE SYSTEMS COMMAND
UNITED STATES AIR FORCE
GRIFFISS AIR FORCE BASE
NEW YORK

VARIAN REPORT NO. 304-1Q

October 1962

Copy No. 32

TABLE OF CONTENTS

LIST OF ILLUSTRATIONS

SECTION I

OBJECTIVES OF PROGRAM

1-1. INTRODUCTION

This report is the first of three quarterly technical notes and one final technical report to be prepared for Rome Air Development Center, Griffiss Air Force Base, New York, under contract No. AF 30(602)-2844. This contract for a "High Power R-F Window Study" was issued 6 July 1962, in accordance with RADC Exhibit "A", dated 29 December 1961.

1-2. OBJECTIVES

A. Primary

The program's final objective is the design of an X-band window with 25 per cent bandwidth and a 250 kw c-w power handling capacity. Design work will include analytical and experimental investigations of various window configurations and dielectric materials under strong multipactor conditions.

Other factors considered to be important in window failures will also be investigated. These include (but are not necessarily limited to) the effect of stray magnetic fields, small variations in gas pressure, merits of gaseous and dielectric window coolants, and the effectiveness of conductive coatings in the reduction of secondary emission on the window faces.

B. First Quarter Objectives

Since this study is a continuation of an effort begun by another contractor, work started where the previous effort had left off, that is, with high power testing of window assemblies. Certain materials for fabrication of window test assemblies were already in the plant, and designs incorporating these materials had already been made. The first objective, therefore, was to complete this work and begin testing with the high power circulator.

In addition to the testing effort, assignments were made to study all of the available literature on window technology which would lead to the design of other window configurations using any necessary dielectrics possessing the desired properties. Requisition of such materials would be of the first order of importance.

Closely coupled to the design of broadband windows is the question of the effect of ghost modes within the dielectric. Effort must be directed to the analysis,

elimination and suppression of these modes because of their proved ability to fracture operating windows.

Other goals to which effort will be directed are the techniques of formulating and applying conductive coatings to ceramics and to the strengthening of their windows by mechanical or other means.

SECTION II

ABSTRACT

Samples of beryllium oxide of various purities, formed by dry isostatic pressing, were obtained and tested for loss tangent, dielectric constant and purity. Fabrication of several windows of the $\lambda_g/2$ block configuration into high power testing jigs resulted in testable pieces which were not vacuum tight.

The ring resonator was used to test the first BeO block windows up to 253 kw of c-w power. Losses in the test section and window were repeatedly measured to be 700 watts, or about 0.3 per cent of the total transmitted power. Temperature gradients in the BeO window were also estimated.

A derivation of the ghost mode distribution in dielectric loaded waveguide was made and a plot of this distribution is shown. This information is to be used in the design of future windows to obtain maximum mode free bandwidth. This bandwidth is not expected to exceed 15 per cent.

Configurations with the most promise of yielding the desired 25 per cent mode free bandwidths are considered to be of the thin disc type. Cold test designs for fused quartz, BeO, Al_2O_3 and BN thin disc windows have been made.

An analysis of the design, fabrication and operation of the dual disc type of configuration has been made. Fabrication of a high power test model of several dual and single disc windows is now in progress.

The investigation of conductive coatings for windows to reduce secondary emission and drain excessive charge from the window face is in progress. The sesquioxide of vanadium is the compound being investigated. Several samples of ceramic have been coated to check its stability and resistivity.

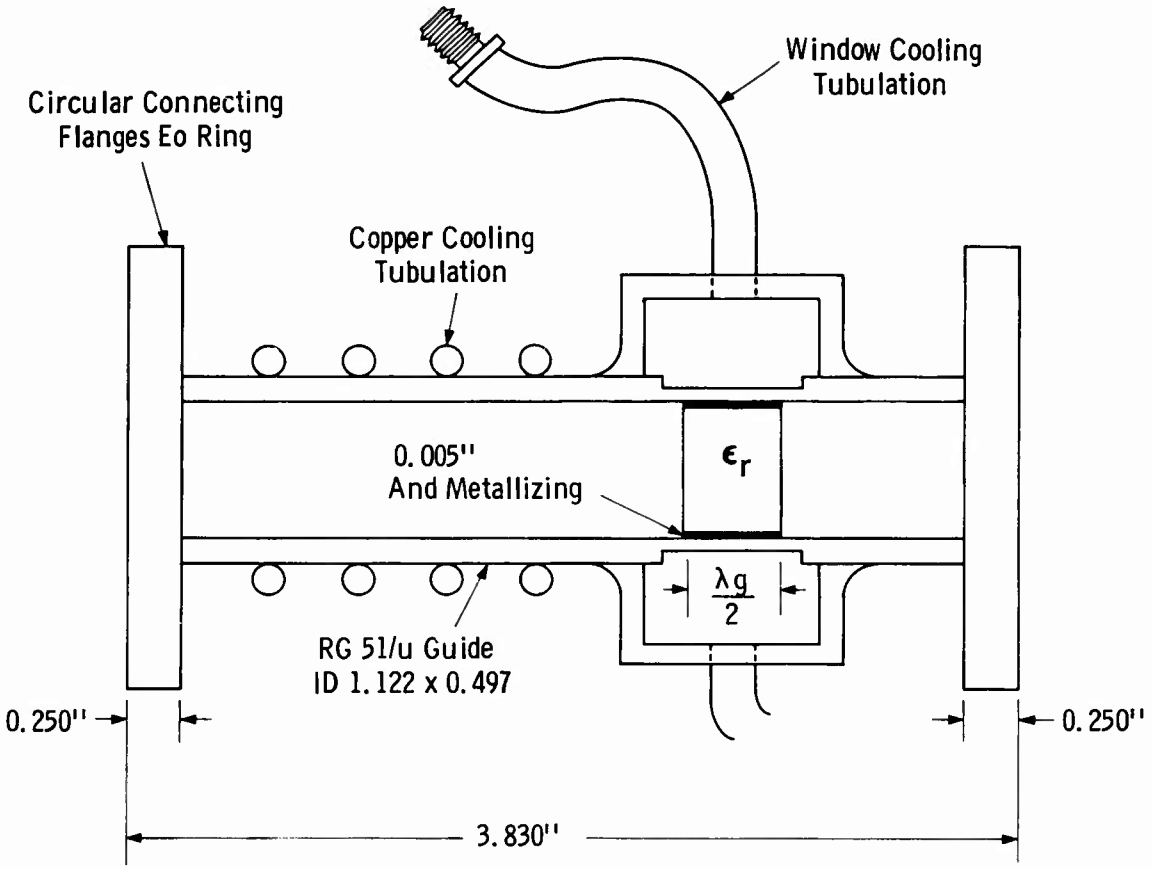

FIGURE 1
HIGH POWER WINDOW TEST ASSEMBLY

SECTION III

TECHNICAL PROGRESS OF PROGRAM

3.1 MATERIALS INVESTIGATION

Three samples of Brush Beryllia's F-7 improved dry isostatically pressed material in the form of rectangular, half wavelength blocks were available at Varian Associates at the beginning of the program. Cold testing had been completed to obtain a VSWR of 1.02 or less at a frequency of 7750 Mc in order that tests could be performed in the X-band circulator at that frequency. Subsequent brazing of these blocks into water cooled assemblies (see Figure 1) showed that all three had minute leaks. Despite these imperfections, it was felt that high power testing would produce useful results.

A minor change in the metallizing procedure has resolved the brazing problem. Vacuum-tight block windows are now being constructed.

Using resonant cavity methods, the dielectric constant of the F-7 body was measured and found to be 6.5 at X-band frequencies. Some indication of shrinkage has been observed during the metallizing process of the ceramic, which naturally increases the relative dielectric constant. The manufacturer can remedy this situation by more carefully controlled firing schedules.

The loss tangent of the F-7 body has been measured at Varian and the material is the lowest loss beryllia yet encountered. Although these measurements were made at S-band, experience has shown that the dielectric loss of most dense ceramics is nearly constant at microwave frequencies. Figure 2 compares F-7 loss with the other ceramics listed in Tables of Dielectric Materials, Vol. V and VI, published by the Laboratory for Insulation Research at the Massachusetts Institute of Technology.

The most recent thermal expansion data on high density BeO are given by Taylor.[1] His expression for expansion from 20° C to 2050° C is

$$\ell = \ell_o \left(1 + 6.95 \cdot 10^{-6} \ (t-25) + 2.17 \times 10^{-9} \ (t-25)^2 \right) \qquad (1)$$

This represents 0.53 thousandths of an inch for a rise of 75° C above room temperature and 9.1 thousandths for a rise of 1025° C, or very nearly that of AL_2O_3.

A sample disc of the F-7 body was X-rayed on a diffractometer in the normal manner for scanning (1° (2θ) per minute). No visible diffraction pattern for impurities was observable for the F-7 body; however, this evidence is not conclusive since certain impurities will not show up under such a process. Samples of Coors BD 96

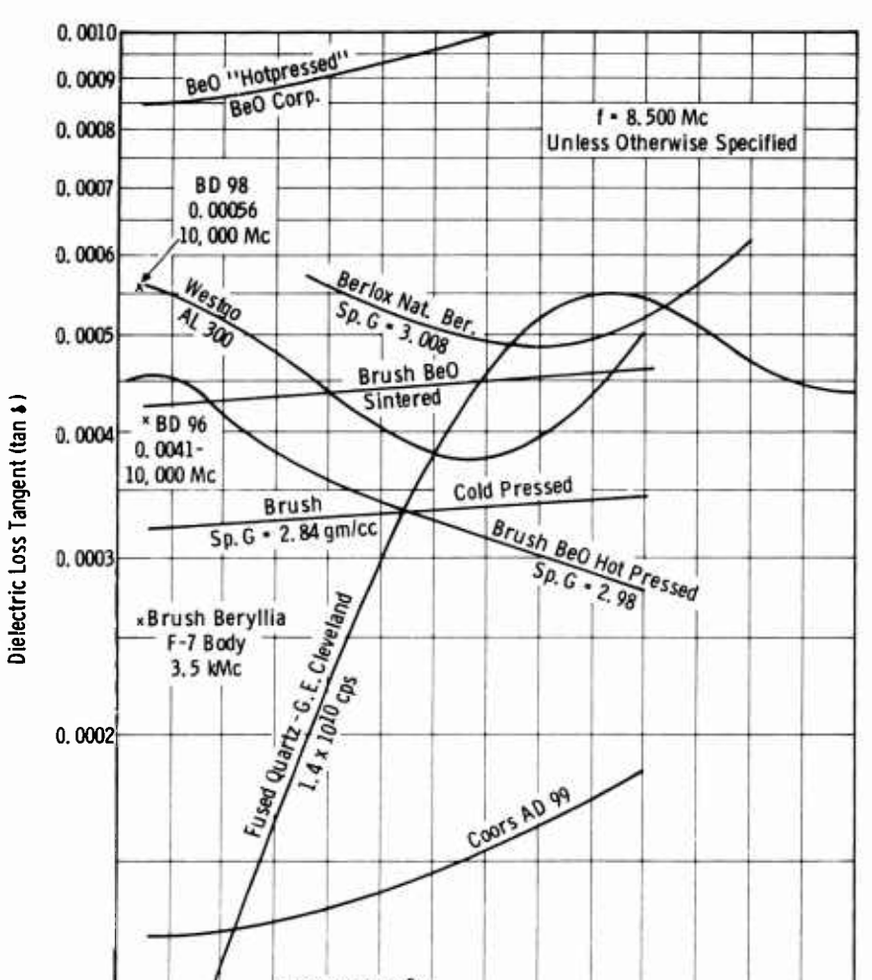

FIGURE 2
DIELECTRIC LOSS TANGENT VERSUS TEMPERATURE
FOR ASSORTED CERAMICS

(a 96 per cent purity) beryllia under diffraction show a spiral structure appearing to be mainly CO_3O_4 but possibly including aluminum in the lattice sites to indicate some CoO AL_2O_3. Samples of Coors BD 98 showed definite indication of Chrysoberyl Be AL_2O_4.

Very little is known of the effect of impurities on beryllia's power handling ability, although it has been shown that small amounts of impurities such as silica and alumina degrade the thermal conductivity considerably.[2]

3.2 WINDOW CONSTRUCTION AND TESTING

A. High Power Testing

The first beryllia $\lambda_g/2$ block window was tested to 253 kw of c-w power in the X-band ring at approximately 2.0 atmospheres of nitrogen. (See Figure 3.) The test frequency was 7762 Mc. No visual failure of the ceramic or damage to the test section was observed. However, r-f arcing damaged the matching hybrid into the ring and pitted the virtual shorting blocks of the output E-H tuner.

These virtual shorts of the input hybrid have been wrapped in teflon tape, while the virtual shorts of the output E-H tuner were redesigned to provide for a contacting short back of the virtual shorting section. Both E-H tuner and hybrid are water cooled, so that I^2R heating on the guide walls does not present any difficulty at present power levels.

After thorough cleaning, the ring was reassembled and the 70 db sampler coupler was recalibrated. This was accomplished in a straight forward manner by measuring power into the coupler by means of a water load and calibrated flow meter. This power was compared to that measured by an HP 431A bridge and barretter. Calibration was made at the 6 kw c-w level. The HP 431A is extremely stable and was operated 10 db above its most sensitive scale to further minimize drift. For convenience, the waveguide attenuator following the coupler was adjusted for a total of 80 db system attenuation so that a 3 milliwatt bridge reading represents 300 kw of ring power.

A power level of 210 kw was readily achieved again in the first BeO window assembly with no attempt to return to the 250 kw level being made. During this test, data were taken to determine simple total test section dissipation versus ring power. This information is presented in Figure 4. The dispersion of the data points at the 250 kw level is due to some thermal instability in the ring resonator. Additional water cooling in the input arm and test pieces has been added and should remedy this difficulty.

The dissipation in the window test sections was made by the standard calorimetric method. The guide section containing the block window is 0.95 inch long. This

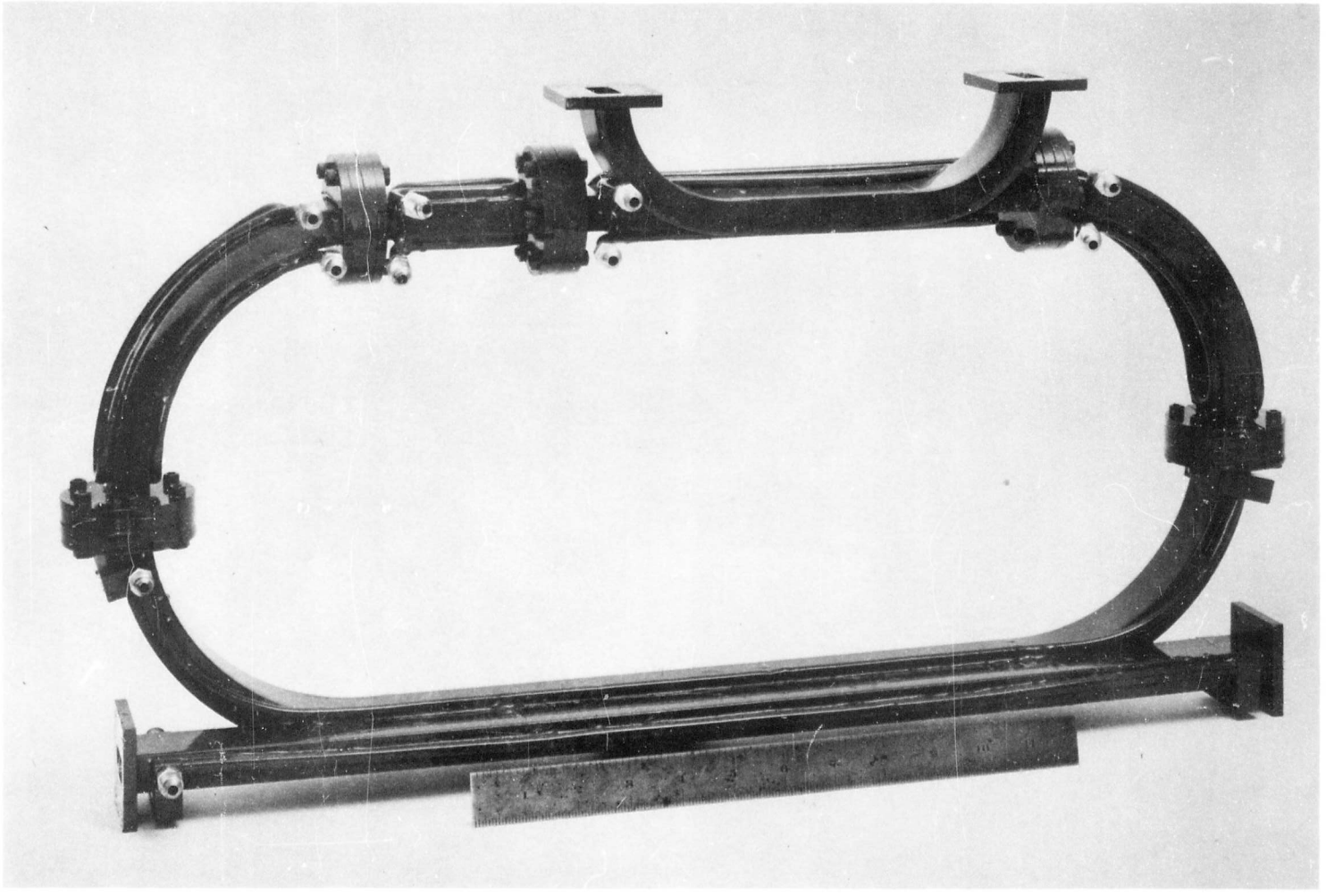

FIGURE 3
HIGH POWER X-BAND RING

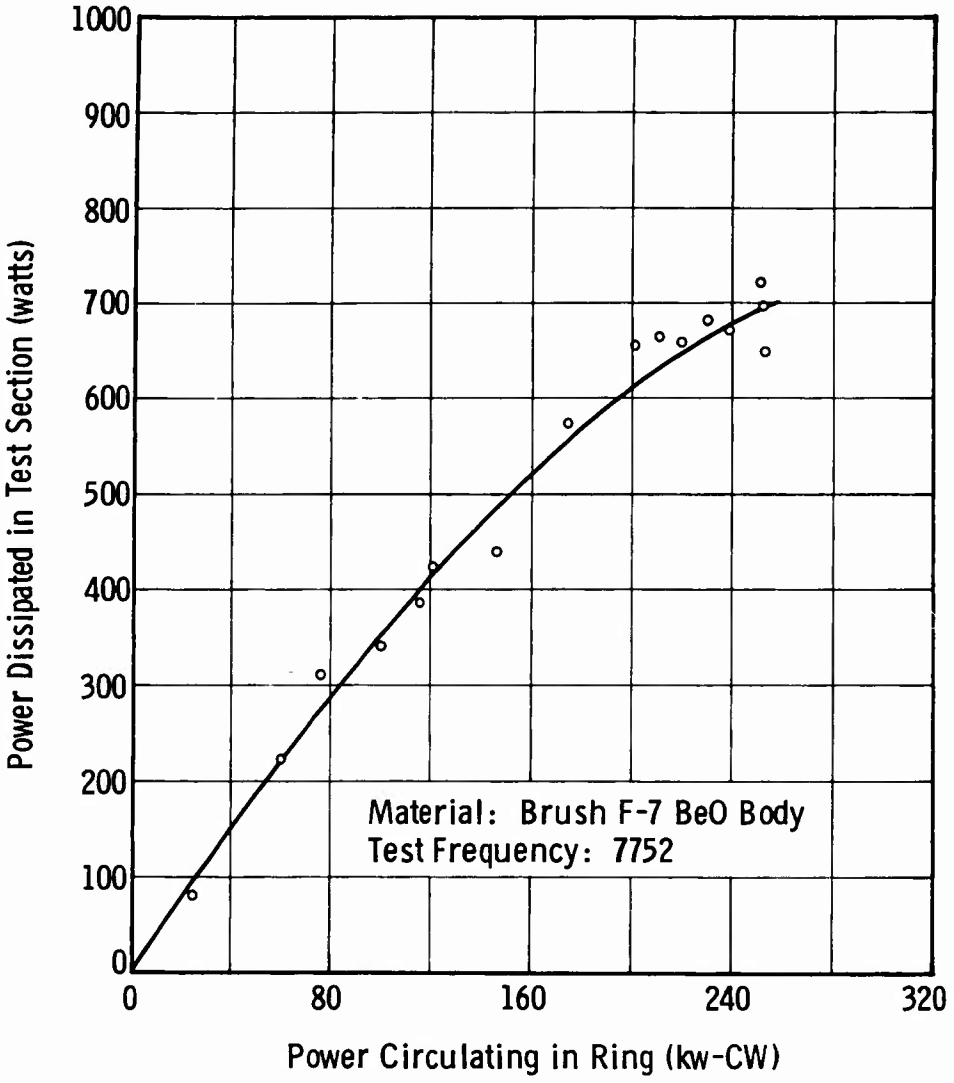

FIGURE 4
HIGH POWER TEST OF BERYLLIUM OXIDE BLOCK WINDOW

length of copper waveguide dissipates 0.003 db, or less than 1/10 of 1 per cent of the power circulating in the ring. At 250 kw this represents 250 watts, or about one third the total measured dissipation in the test section.

Beryllia windows Nos. 2 and 3 have been tested up to 130 kw to confirm the first window dissipation versus ring power curve, and at the same time to provide temperature rise information. The method used to estimate the temperature rise across the face of a window ceramic involved a crayon-like material which melts at or above a pre-determined temperature. Thin layers of this material (tempelstik) may be applied to the surface of the window without appreciably changing the electrical properties of the window. By careful measurement of the guide wall temperature with embedded thermocouples, the temperature rise across the window at a given power level can be estimated by measuring the width of the temperature contour presented by the melted tempelstik. Adjustment of flow rate and appropriate choice of tempelstiks permit measuring contours for several guide wall temperatures until a combination is reached with no melting. This point represents an upper limit to the window temperature. The tempelstik has been applied both as thin strips and polka-dots and has produced essentially the same results as the thin layer covering the whole window surface. Results of the tempelstik experiments on the first beryllia block window show a temperature rise of about 60 per cent of a comparable high density alumina. Figure 5 shows the typical melting contours obtained. The contours represent cooling and remelting of the tempelstik as the ring and window test assembly were operated up to 253 kw cw. Maximum heating of the window at the high field point is indicated, as would be expected.

The first beryllium block windows were constructed as simply as possible to provide data which could be compared readily to that of existing windows at Varian. These windows were a half wavelength long and provided a VSWR of less than 1.05 at 7762 Mc. As calculated, no ghost mode resonances were observed within the narrow pass band of these windows. However, since the high electric fields associated with several of the ghost mode resonances are thought to be one of the mechanisms of high power window failure, it was decided to compute the resonances for several block windows of various aspect ratios at X-band. By computing the modes (see Appendix), a search can easily be made for potential areas of safer broadband operation.

Appendix Equations (11) and (15) have been programmed for digital computation. Point by point solutions of the transcendental pairs, made by the computer to find exact frequencies of resonance, are plotted in Figure 6. The error in the extrapolation process is extremely small as may be noted by observing the well-behaved characteristics of the transcendental sets in the range specified. Experience at Varian has shown that calculated resonances agree within 1 per cent of the measured resonance when dielectric constant is known accurately and construction tolerances are properly maintained.

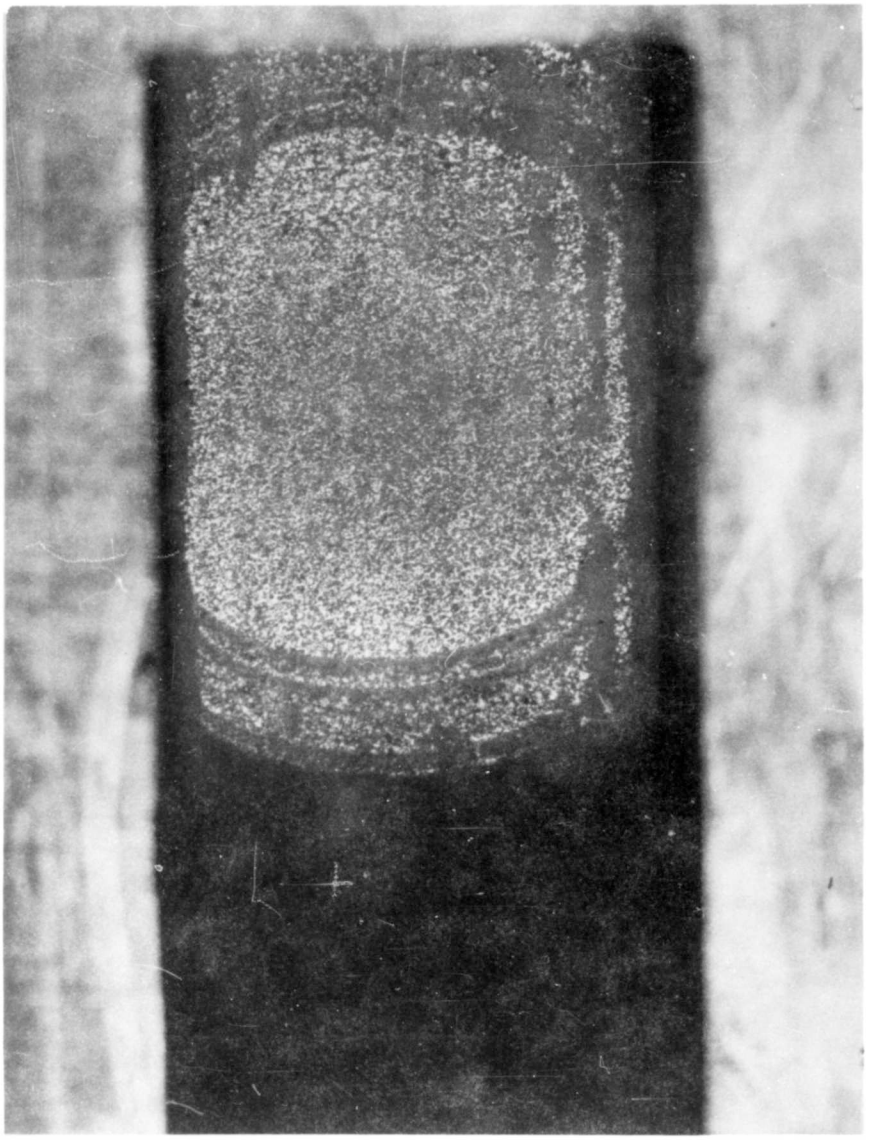

FIGURE 5
TEMPELSTIK MELTING CONTOURS ON BERYLLIUM
OXIDE BLOCK WINDOW

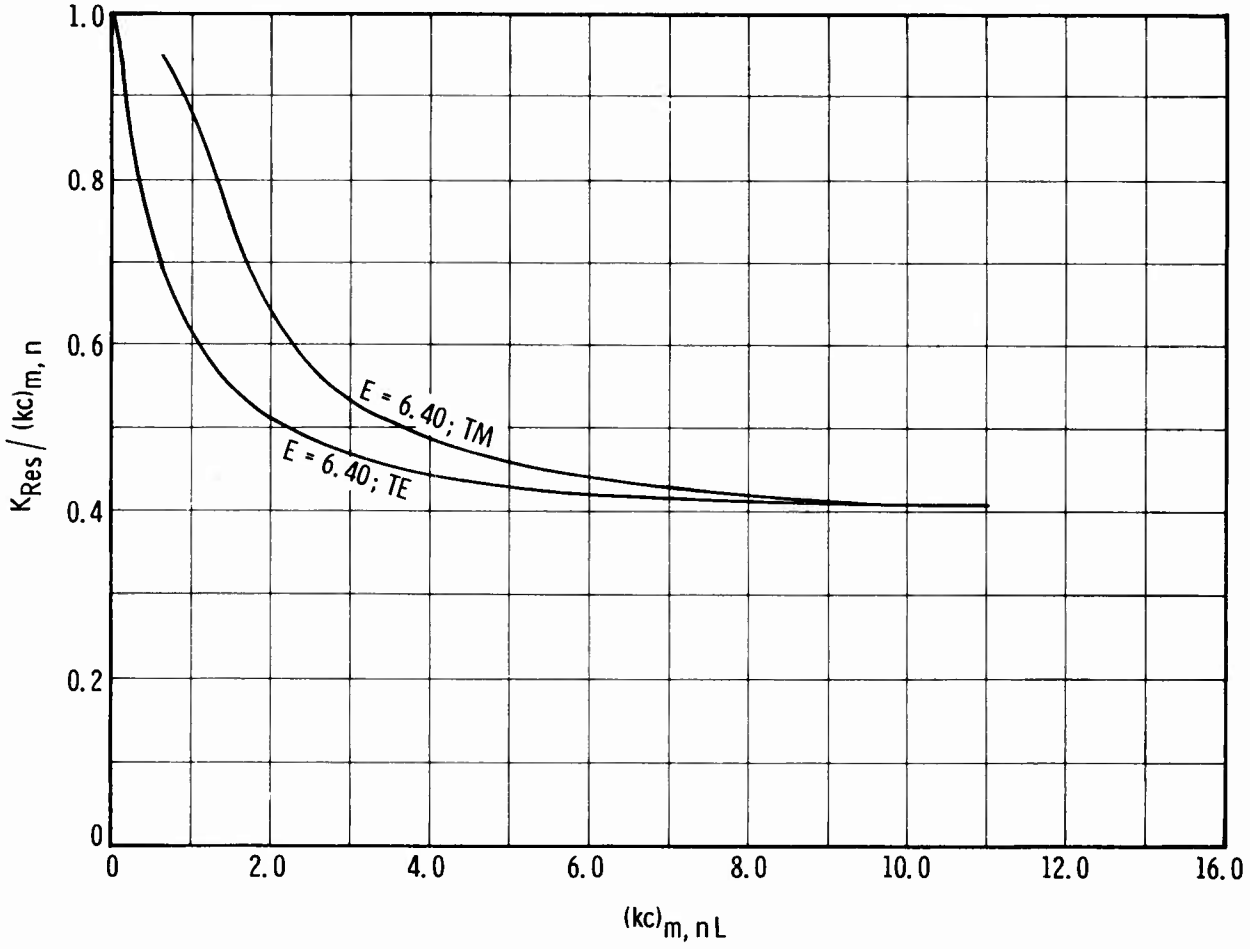

FIGURE 6
GHOST MODE SOLUTION CHART

B. Configuration Study (Single Disc)

As indicated in the derivation of the ghost mode resonances in the Appendix, windows with all currently favored configurations will have these modes distributed throughout the band to a greater or lesser extent. In particular the thick, $\lambda_g/2$, windows have an extremely dense distribution of ghost modes which makes broadband design of ghost mode free windows in this configuration very difficult, if not impossible. Perhaps 10 or 15 per cent mode free bandwidth is all that can be expected from such designs. For high power amplifiers with bandwidths not in excess of these percentages, thick X-band windows using beryllium oxide ceramic have been shown capable of transmitting 250 kw of c-w power. A 25 per cent mode free bandwidth presents quite another problem. Here, thick half wavelength ceramics cannot presently be used until some method of mode suppression is found. Therefore, thin ceramic shapes currently offer the best possibility for success because of their larger mode separation characteristics.

With these considerations in mind, the design for matched, mode free thin windows was pursued more aggressively than any other configuration during this period. Dielectric materials thought to exhibit desirable properties as waveguide windows were ordered. These include single crystal (zero degree cut) sapphire, aluminum oxides (AL 995, AL 400, AL 300), beryllium oxides, fused quartz, and boron nitride. The latter two materials have one very undesirable property in common, their low thermal expansion. Use of fused quartz windows has been considered by several window studies during the past few years, but no concrete conclusion has been put forth concerning whether use of this material should be seriously pursued. This study will investigate whether fused quartz works well as high power microwave windows. (The fact that reliable vacuum-tight seals have not been developed can be bypassed if necessary for such tests.) If the answer is in the affirmative, then some firm recommendations will be forthcoming on whether, and perhaps how, to pursue the vacuum sealing problem.

Most of the materials discussed have been delivered, and cold tests have begun on all of them with results which follow. It should be noted in this discussion that the bandwidth is taken as that range of frequencies over which the VSWR of the device is 1.2 or less.

1. Single Thin Disc Sapphire

The Linde single crystal sapphire discs, 1.4 inches in diameter and 0.050 inch thick, were cold tested without success because of the unexpected and unrepeatable results. Further investigation revealed that these crystals were not really zero degree cut and therefore exhibited different properties, depending on the discs orientation in the waveguide. They are being returned to the manufacturer for replacement.

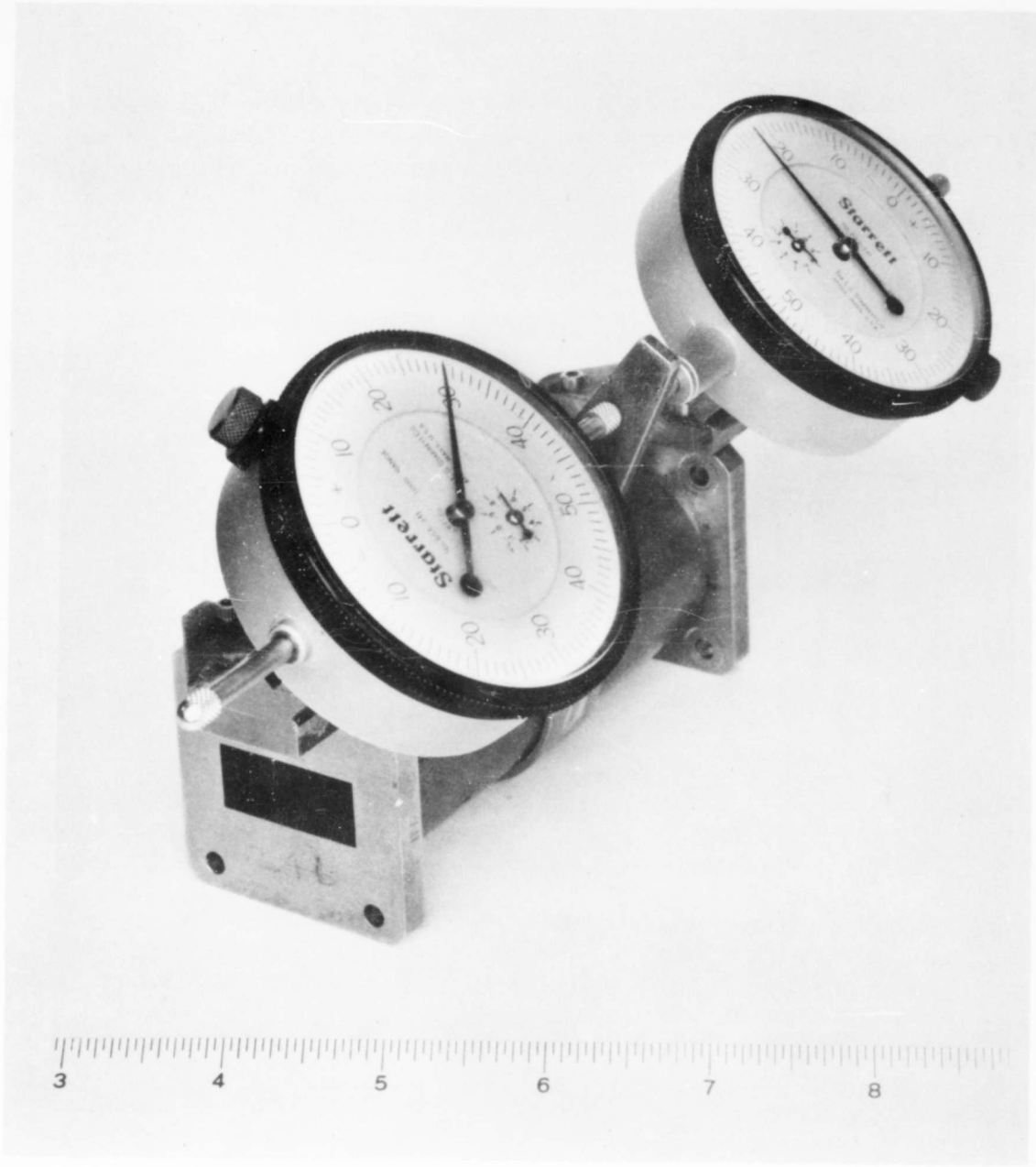

FIGURE 7
COLD TEST JIGGING FOR THIN DISC WINDOWS

2. Single Thin Disc Quartz

Figure 7 shows the cold test jigging used in testing all of the thin disc windows to date. This device allows continuous tuning of the cavity length for optimum match with a repeatable accuracy of 0.002 inch in cavity length. Only preliminary tests have been performed with the quartz window. The results are shown in Figure 8. The bandwidth for this window is a fair 23.7 per cent where no optimization of window parameters has been attempted. All that is necessary for high power tests is a device well matched at the initial test frequency of 7750 Mc. If fused quartz should prove to be desirable for transmission of high power, further impedance matching will be done. Several ghost mode frequencies are indicated in Figure 8. Although they do not always affect the reflected power to any appreciable extent, it can be safely assumed that in high Q resonances (1000 to 2000) considerable energy is stored, creating a dangerous situation when transmitting high average powers at a frequency near the resonance.

3. Single Disc Aluminas

Single disc alumina windows have been used extensively at Varian Associates. A patent (No. 2958834) for such a window was issued to R. Symons and A. Schoennauer of Varian in 1960. The art of designing and building such windows is fairly well known throughout the tube industry and no effort will be directed toward improving this window as such. However, it is introduced here to demonstrate the ever present ghost mode situation. Figure 9 displays the results of first measurements of VSWR when a paper design is assembled in the cold test jigging. Without optimization of any kind, the VSWR is better than 1.2 across the entire band. At least six major ghost modes can exist in this window with these dimensions. Past experiments have shown that a maximum of 16 per cent mode free bandwidth can be obtained in this configuration using alumina ceramics.

4. Single Disc Boron Nitride

A relatively new material presently being suggested for use as waveguide windows is boron nitride. A selected summary of the published properties pertinent to waveguide windows is shown in Table I.

Several interesting properties of this material are the low dielectric and loss tangent constants and the high thermal conductivity in the "a" direction. The low dielectric constant could mean a design of a more mode free window because these resonances are a function of dielectric constant. The low loss tangent is desirable to reduce losses, and thus, heating, to a minimum. The heat that is generated can be more easily removed because of its high thermal conductivity when using circumferential cooling.

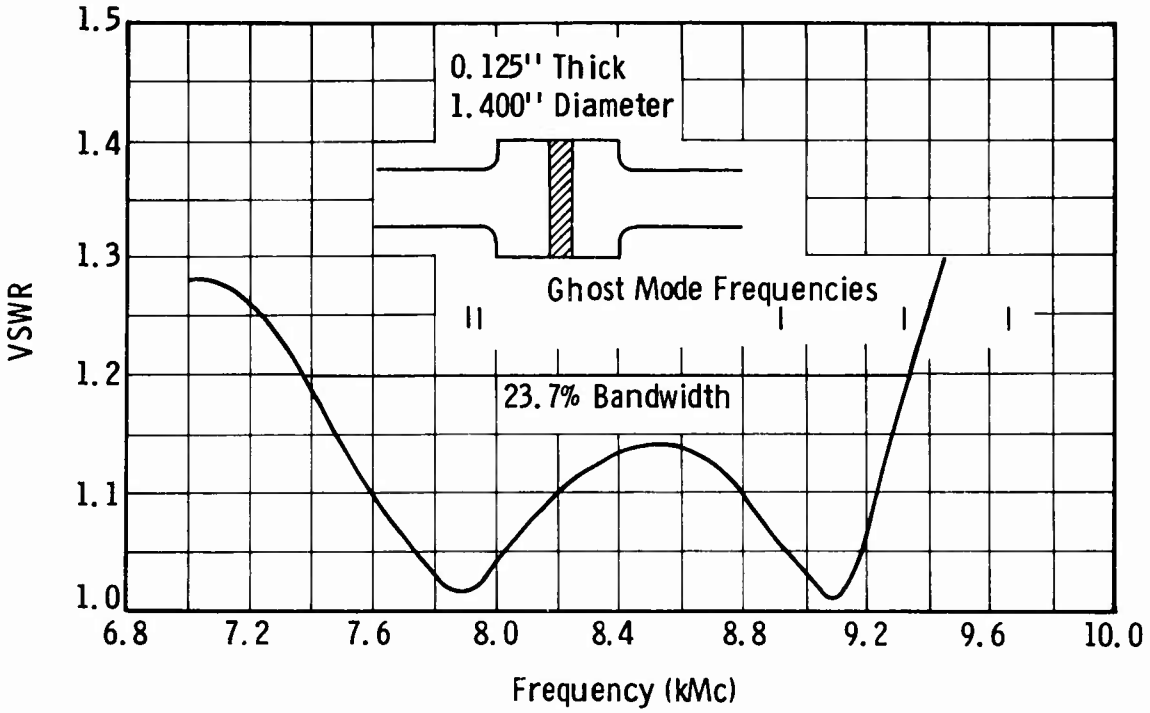

FIGURE 8
SINGLE DISC QUARTZ WINDOW CHARACTERISTICS
VSWR VS FREQUENCY

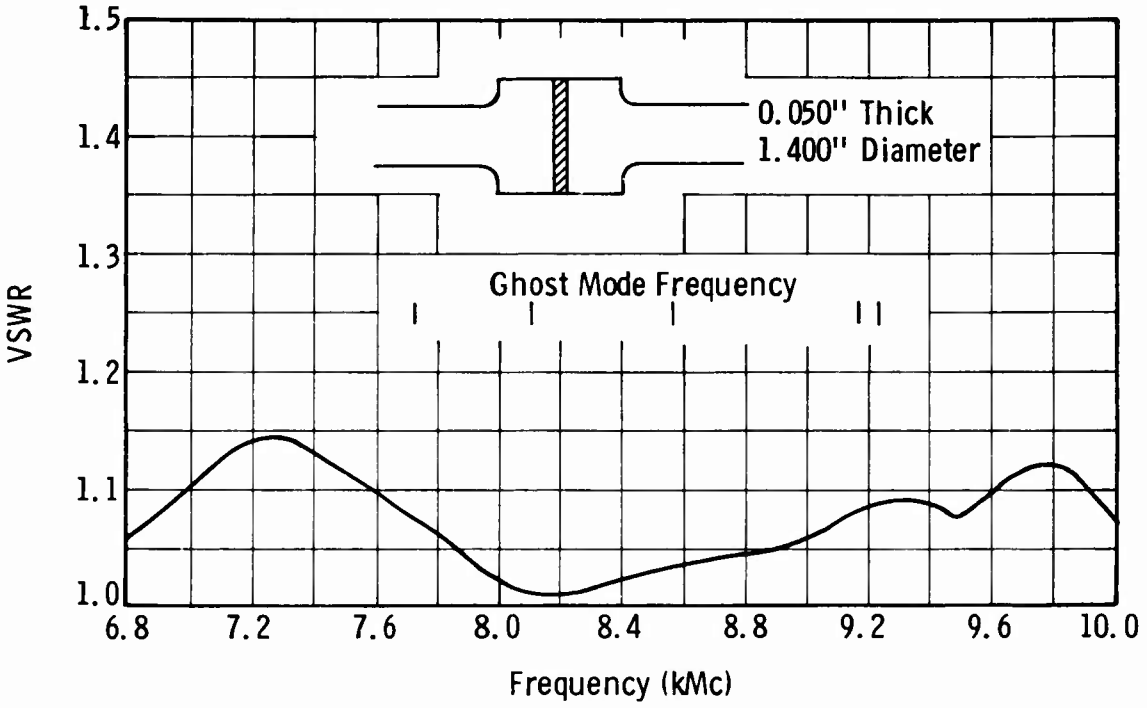

FIGURE 9
SINGLE DISC AL 300 WINDOW CHARACTERISTICS
VSWR VS FREQUENCY

TABLE I

PROPERTIES OF BORALLOY*

Crystal structure	Highly oriented polycrystal
Porosity	0 per cent
Thermal Conductivity	0.004 in "C" direction
	0.4 in "a" direction
Thermal expansion	25×10^{-6} in "C" direction
	1×10^{-6} in "a" direction
Youngs Modulus (25° C)	4×10^{6} psi in "a" direction
Flexural strength (25° C)	15000 psi in "a" direction
Relative dielectric constant 25° C	5.12 in "a" direction
	3.40 in "C" direction
Loss Tangent (4 kMc)	0.00015 in "a" direction
	0.0001 in "C" direction

"C" is normal to the surface of the window

"a" is parallel to the surface of the window

The low thermal expansion in the "a" direction and the low strength of boron nitride indicate that problems similar to those experienced with fused quartz may preclude its use in waveguide windows.

Samples of Boralloy were obtained and cold tested. The results are shown in Figure 10. The matched bandwidth obtained is somewhat narrower than that seen with other materials, but with variation of a few of the configuration parameters it could undoubtedly be improved. As can be seen from the figure, ghost mode resonances appear to be numerous in this material also.

- - - - - - -

*Trademark of High Temperature Materials, Inc., for pyrolytic Boron Nitride.

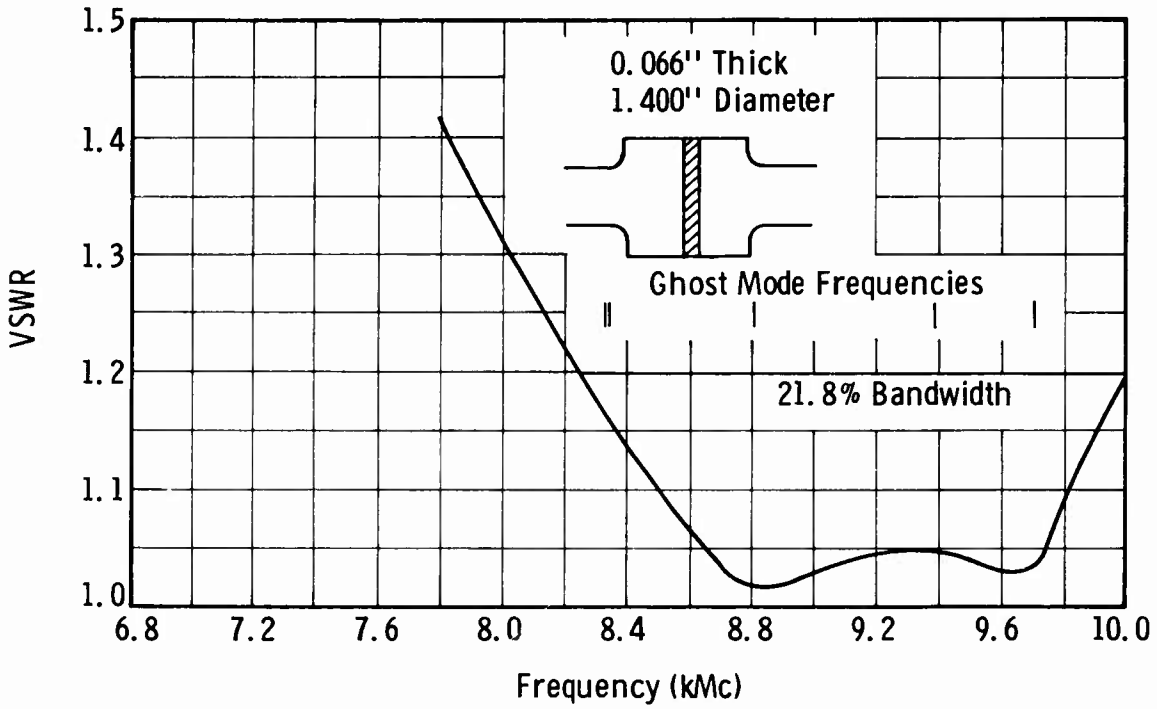

FIGURE 10
SINGLE DISC BORON NITRIDE WINDOW CHARACTERISTICS
VSWR VS FREQUENCY

C. Configuration Study (Double Disc)

Thin disc windows often have less mechanical strength than desired. They are generally constructed simply by metallizing and brazing the dielectric into a cylindrical waveguide. These seals are often broken in tube bakeout or during high power operation when over-heating is experienced. Excessive waveguide pressurization also may cause ceramic fracture. These failures caused by mechanical failure of the window dielectric could often be prevented by more careful design. In particular, two methods of such strengthening are suggested and will be investigated. These are ceramic glazing, and the use of metal hoops brazed around the circumference of the disc ceramics and to the waveguide wall.

The hoop support is shown in Figure 11. With the ceramic metalized and brazed to the hoops, the assembly has much more support. Without the support it could be assumed that the equations for flat plate loading,[3] edges supported, uniform load, are good approximations.

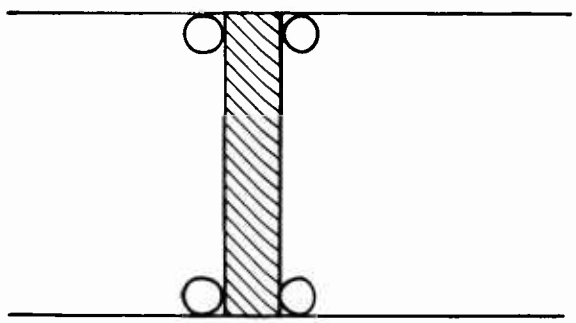

FIGURE 11
BRAZED THIN DISC WINDOW, HOOP SUPPORTED

At the disc center $W = \omega \Pi a^2$

$$Y_1 \max = \frac{3W (m - 1) (5M + 1) a^2}{16\Pi E M^2 t^3} \quad (1)$$

$$S_1 \max = \frac{3W (3M + 1)}{8\Pi M t^2} \quad (2)$$

With the hoops brazed in the cup and to the ceramic the equations for flat plate loading, edges fixed, uniform loading, are approximated.

At disc center $W = \omega \Pi a^2$

$$Y_2 \text{ max} = \frac{3W (m^2 - 1) a^2}{16\Pi E m^2 t^3} \quad (3)$$

$$S_2 \text{ max} = \frac{3W (m + 1)}{8\Pi m t^2} \quad (4)$$

where

a = disc radius in inches

t = thickness in inches

S = stress in psi

W = total load in pounds

ω = pressure

m = 1/Poissons ratio = 3.3

Y = deflection in inches

E = Youngs modulus in psi

In the ideal case, the ratio of $S_1 \text{ max}$ to $S_2 \text{ max}$ will give the factor by which the hoop supported window is stronger than the non-supported window.

$$\frac{S_1 \text{ max}}{S_2 \text{ max}} = \frac{(3m + 1)}{(m + 1)} = 2.5 \quad (5)$$

Similarly the ratio of $Y_1 \text{ max}$ to $Y_2 \text{ max}$ gives an indication of the larger deflection in the non-supported case. This would undoubtedly cause an impedance mismatch since the average deflection of 3.2-inch diameter windows has been measured to be 0.010 inch just before fracturing.

$$\frac{Y_1 \text{ max}}{Y_2 \text{ max}} = \frac{5m + 1}{m + 1} = 4.1 \quad (6)$$

A series of measurements were taken using the device shown in Figure 12. Using 3.22- and 1.32-inch diameter AL 300 ceramic discs brazed into copper cups, this device allowed measurement of pressure exerted and total deflection in the ceramic as pressure was increased. With the diameter-to-th.ckness ratio constant, the resulting data plotted in Figure 13, show that the hoops do strengthen the assembly by at least a

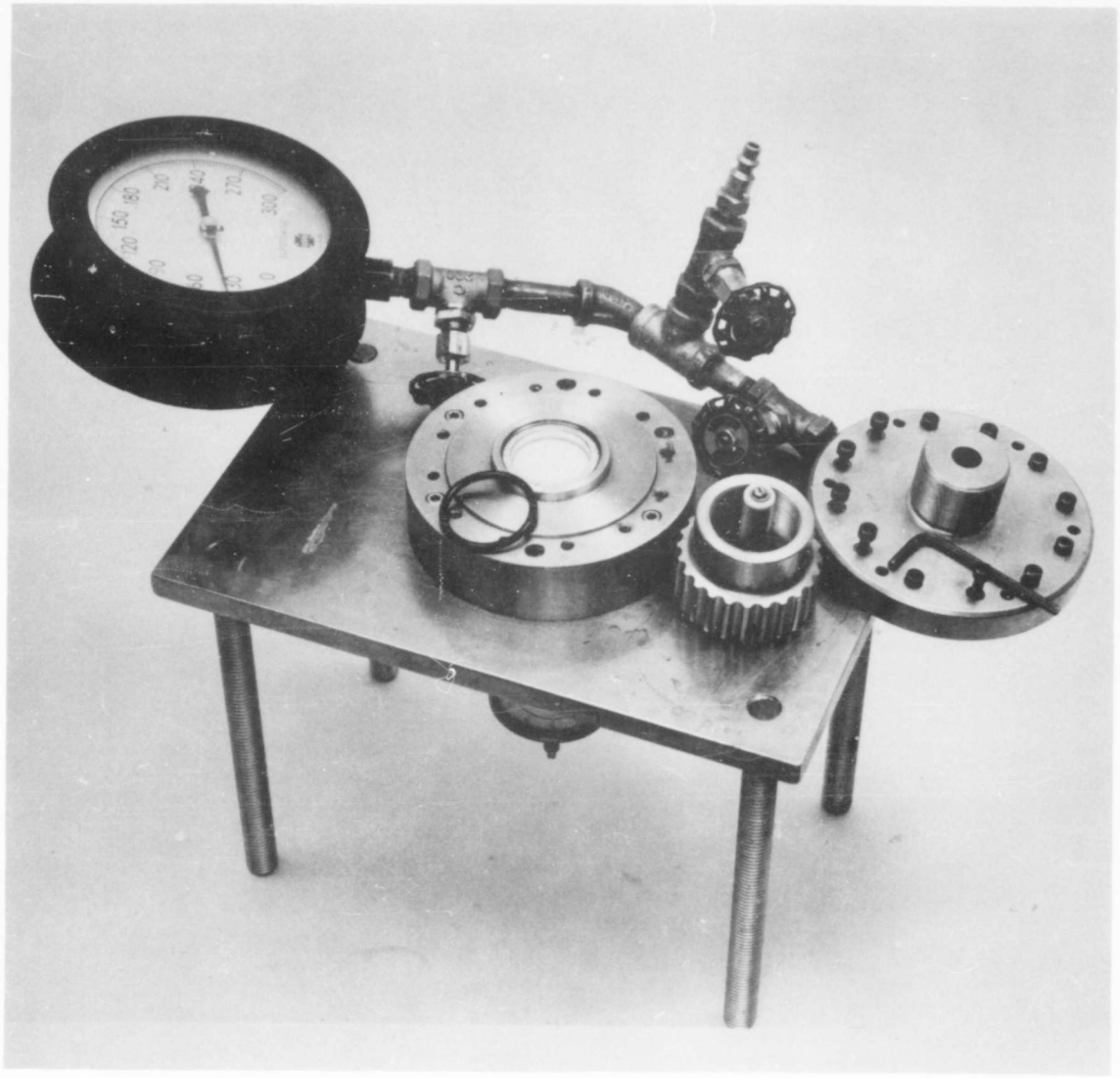

FIGURE 12
FRACTURE TESTING ASSEMBLY

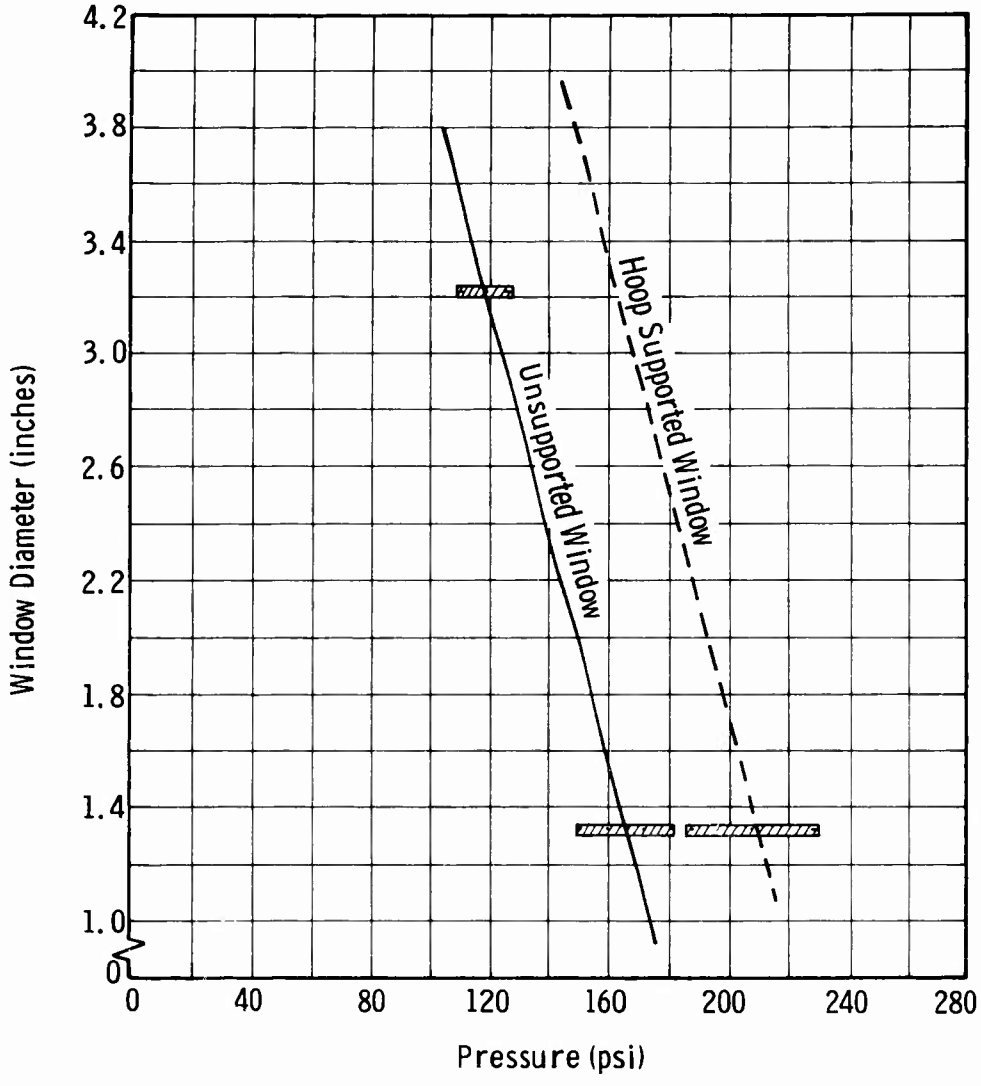

FIGURE 13
FRACTURE REGIONS OF AL 300 DISCS - DIAMETER VS PRESSURE

factor of 1.3. The number of samples of hoop supported windows broken was small and the hoop brazes were very poor. As the technique for making these brazes improves, the fracture point is expected to show an improvement of about two times that of an unsupported disc.

Electrically these hoops have been shown to affect the window match only slightly. Although no windows of this type have yet been tested in the ring circuit, it is expected that the voltage breakdown problem will not be increased by the use of hoops, since no sharp edges are exposed to the electric field. In fact, the hoops will cover the sharp feather edges of braze fillets, as often seen in thin disc windows, and could improve the window in this respect.

No work has yet been done to determine if any improvement in strength is obtained by a ceramic glazing process.

The thin disc strength problem is further aggravated in double disc windows because the discs will generally be thinner in order to get the broadest bandwidth possible. For example, if the thickness of any given pressurized window is halved, the stress generated is four times as great. Any factor of safety which is obtained by the schemes suggested is then much desired.

The major advantage of the double disc window is the ease with which it can be cooled. A cooling liquid such as FC 75 can be injected through a slot as shown in Figure 14. In this way a minimum amount of wall current, J_z (about 10 per cent maximum), is intercepted if the slot arc does not subtend an angle greater than approximately $\pm$ 6°.

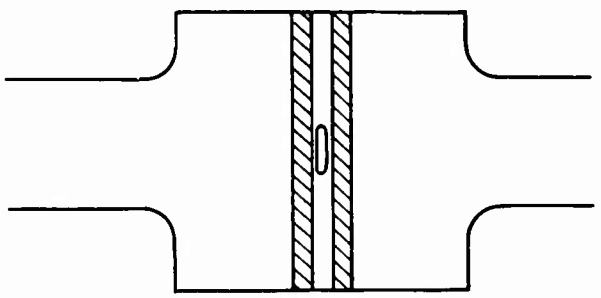

FIGURE 14
DOUBLE DISC WINDOW WITH COOLING SLOT

The power losses within the ceramic can be calculated using the following equations:

$$\alpha = \frac{k}{2} \frac{\epsilon''}{\epsilon' \sqrt{1 - (f_c/f)^2}}$$

$$P_{lost} \simeq 2 \alpha P_{in} \ell$$

where

ϵ' = dielectric constant

ϵ' (AL 300) = 9.04, ϵ' (FC 75) = 1.86

$\frac{\epsilon''}{\epsilon'}$ = loss tangent

$\frac{\epsilon''}{\epsilon'}$ (AL 300) = 0.00045, $\frac{\epsilon''}{\epsilon'}$ (FC 75) = .009

f = 8.5 kMc

$k = \frac{2\Pi}{\lambda_o} \sqrt{\epsilon'}$

$f_c = \frac{0.293C}{a \sqrt{\epsilon'}}$

P_{in} = 250 KW

ℓ = 0.050 for both dielectrics

The losses in the FC 75 have been calculated to be 700 watts with an input power of 250 kw. Losses in the window material are also calculated to be approximately 70 watts or 1/10th of the coolant losses. This indicates that the spacing between thin windows must be kept to a minimum and that an adequate fluid flow must be maintained.

Using the specific heat and density of FC 75,

$$G = \frac{H}{115.8 \times \Delta T}$$

where

$G = \frac{\text{gallons}}{\text{minute}}$

H = power in watts

ΔT = temperature difference between coolant input and output

the necessary flow rate through a window for a given temperature rise and power loss can be determined.

Head loss, flow and pressures are other considerations entering into the design of double disc fluid cooled windows. An analysis of the fluid flow problem has been made and is shown in the Appendix.

The results show that for a fluid flow of 0.5 gal/minute, the pressure on the window will be about 20 psi. Such a flow will cause a temperature rise across the window of about 17° C with a total dissipation of 1000 watts.

The dielectric constant of FC 75 is 1.8 at 8.5 kMc and its loss tangent is 0.009. It is also very expensive - - $135 per gallon. Any amount of loss of this fluid would be prohibitive. In cold testing it would be difficult to use and still have a rapid means of varying the window parameters for a match. Therefore, a search was made for an easy-to-use, inexpensive substitute for FC 75 in cold testing. It was found that a substance made by Emerson and Cumming, Eccostock R20, had close to the desired dielectric constant (1.9) and a loss tangent of 0.008. Figure 15 illustrates the effect of R20 on AL 300 dual disc windows matched for the broadest band of operation in each case. A double disc AL 995 has also been cold tested with results practically identical to that of the AL 300.

Results of cold tests using beryllium oxide dual discs are shown in Figure 16.

A 5 kw FC 75 heat exchanger is scheduled for delivery in October 1962 for use in high power testing of the dual disc windows.

D. Conductive Coatings

The objective of the investigation of conductive coatings for high power R-F windows is to increase power handling capacity by draining excessive charge accumulation on the surface and reduce secondary emission. The charge build-up of electrons can lead to arcs and failure of the window dielectric. High secondary emission coupled with r-f energy can result in further bombardment of the window leading to excessive heating and thermal shock failure.

The following criteria for a conductive coating material have been adopted:

1. Low vapor pressure
2. Stability in vacuum and hydrogen brazing atmospheres
3. Reproducible resistivity under vacuum tube processing conditions
4. No cathode toxicity

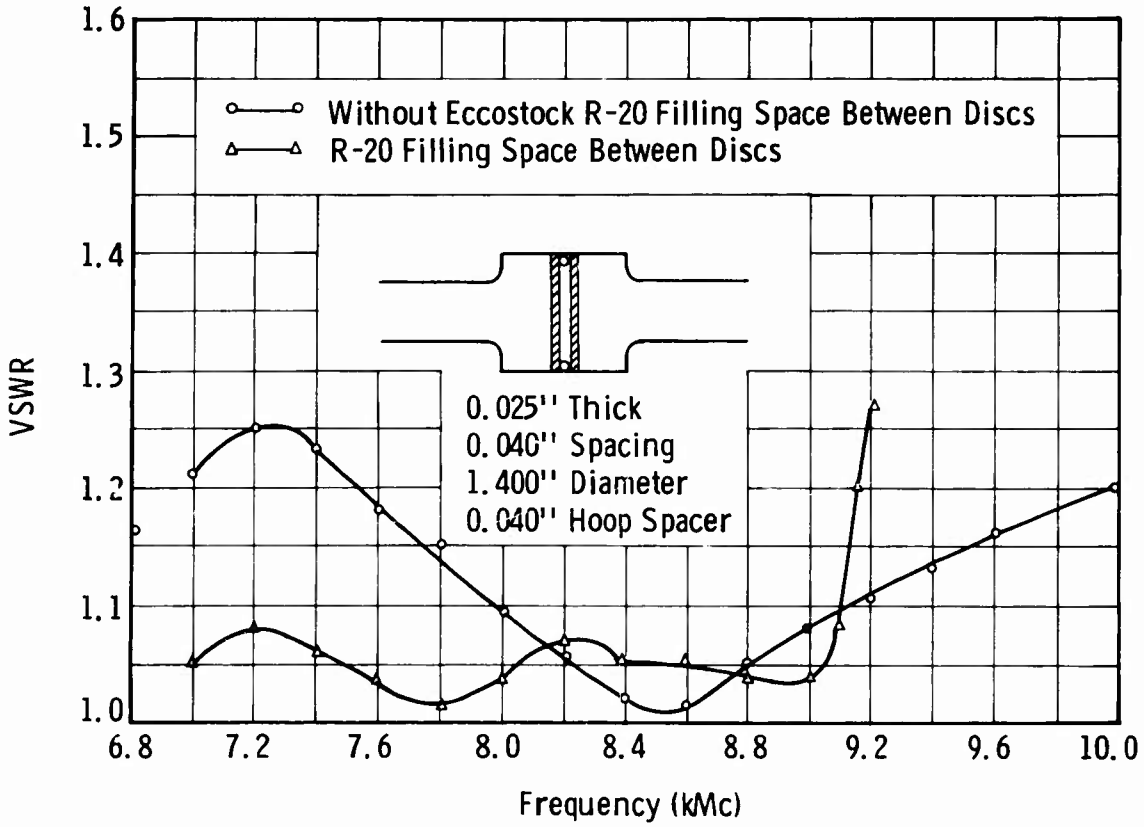

FIGURE 15
DOUBLE DISC AL 300 WINDOW CHARACTERISTICS
VSWR VS FREQUENCY

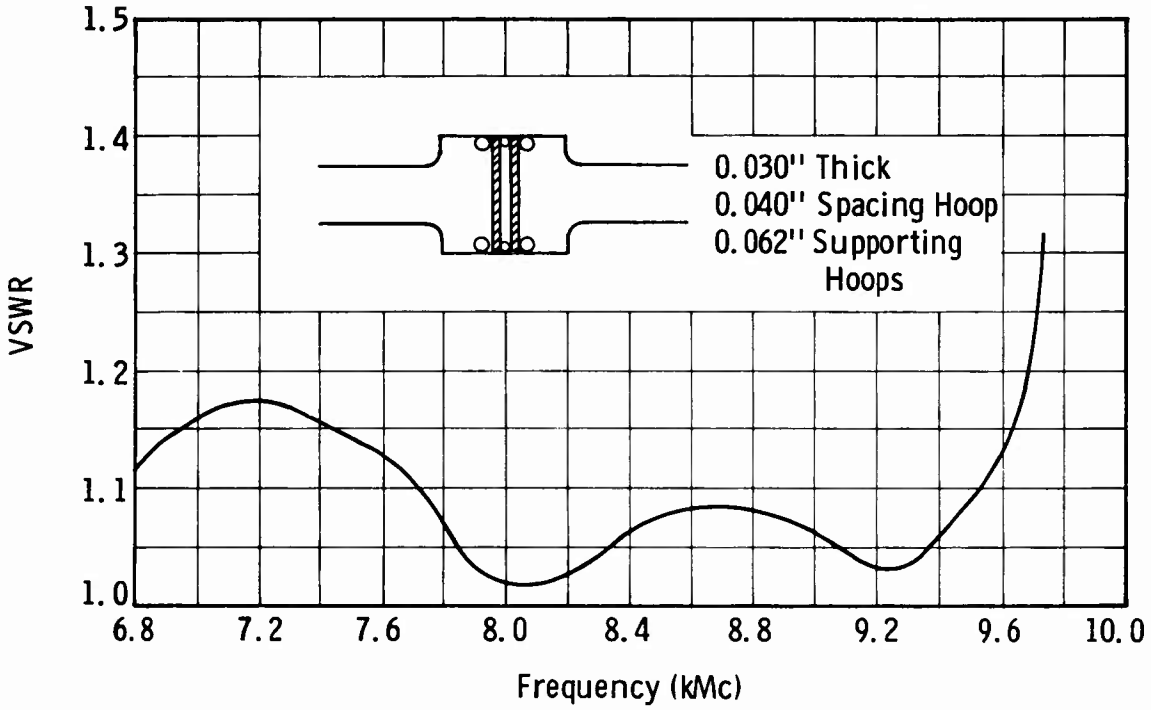

FIGURE 16
DOUBLE DISC BeO WINDOW CHARACTERISTICS
VSWR VS FREQUENCY

5. Good bondability to dielectric substrate

6. Low loss in microwave frequency fields

7. Coating resistance in range of 1 megohm/sq.

Semiconductors as a class of materials seem most likely to meet the criteria for conductive window coatings. These materials have low secondary emission and electrical resistivity which can be adjusted over large ranges by suitable doping agents. Our experience indicates that most thin metal film coatings are not very stable under tube processing conditions. Glasses that depend on ionic conduction are in many cases not stable under tube processing and may produce undesirable electrolitic effects.

The sesquioxide of vanadium V_2O_3 was selected for this coating work since it appears to meet most of the requirements for a conductive window coating. V_2O_3 prepared by the hydrogen reduction of V_2O_5 is a very stable oxide with a melting point of about 1900° C. It appears to be stable in wet hydrogen at our metalizing temperatures (1500 - 1600° C). With respect to cathode toxicity, there seems to be very little possibility of poisoning from V_2O_3. The vapor pressure of the compound seems to be quite low, so that bakeout at 600° C should be feasible. Experiments to date indicate that bondability of V_2O_3 to 97.6 per cent alumina is very good. Reproducibility of resistivity of V_2O_3 coatings on alumina has been good. Several samples in the range of one megohm/sq. have been produced.

Since α Al_2O_3 and V_2O_3 are structurally isomorphous we may expect high bond strengths with alumina ceramics. The oxide V_2O_3 may be considered a degenerate semiconductor, that is, its electrical properties are in part metallic in nature. This property of V_2O_3 will allow control of its electrical properties over a very wide range by adding a semiconductor that enters into solid with the oxide.

The sesquioxide of chromium meets all the requirements for a doping agent for V_2O_3. The chromium oxide Cr_2O_3 is isomorphous with both V_2O_3 and α Al_2O_3. Thus, by means of continuous series of solid solutions we should be able to achieve a wide range of electrical properties. Since all three oxides α Al_2O_3, V_2O_3 and Cr_2O_3 are very stable oxides we can expect to produce very stable resistive coatings.

Our work to date has evolved firing coatings of V_2O_3 on 97.6 per cent alumina ceramic using various coating methods. Hand painting V_2O_3 suspended in nitrocelluose-amylacetate solutions did not yield controllable thickness of coatings. The silk screen method for coating windows shows considerable promise. To date, however, the most uniform and repeatable coatings have been produced by spray methods. Samples fired at 1500° C for 30 minutes exposed to room air for five months have shown no change in resistance.

We plan to prepare a fresh batch of V_2O_3 since the material now in use was made over a year ago and X-ray analysis indicates that the V_2O_5 was not completely reduced. Test windows will be coated with the new pure V_2O_3 for r-f loss measurements. Additions of Cr_2O_3 to V_2O_3 will be made to determine the range of controlled resistance and r-f loss. Windows will also be prepared for high power testing.

3.3 REFERENCES

1. Taylor, R. E. "Thermal Conductivity and Expansion of Beryllia at High Temperatures," Journal of the American Ceramic Society, v. 45, No. 2, (February 1962) pp. 74-78.

2. Day, R. K. Report prepared for Brush Beryllia on "Thermal Conductivity of Beryllium Oxide of Various Purities," (July 11, 1962).

3. Roark, R. J. Formulas for Stress and Strain, 3rd ed. McGraw-Hill, New York, 1954, pp. 194-195.

4. Staprans, A., and Mercer, S. L. Unpublished paper prepared for Varian Associates, February 1962.

5. Ramo, Simon, Whinnery, John R. Fields and Waves in Modern Radio, John Wiley and Sons, New York, 1960.

6. Forrer, M. P., Jaynes, E. T. "Resonant Modes in Waveguides Windows," IRE Transactions on Microwave Theory and Techniques, v. MTT-8, No. 2, (March 1960) pp. 147-150.

7. Vennard, J. K. Fluid Mechanics, 3rd ed., John Wiley and Sons, New York, (1957) p. 216.

SECTION IV

FISCAL STATUS OF PROGRAM

The rate of expenditure on the High Power R-F Window Study Program has been approximately $5,900 per month. This includes about $380 per month spent on materials for window construction and small components. The number of man hours expended during the first quarter was 1388, not including the effort directed to writing and producing the first technical note. These figures are somewhat lower than the amount budgeted, largely due to the late contract issuance date.

It is expected that the expenditure rate will increase slightly during the coming quarter to cover increased fabrication and testing of various window configurations.

SECTION V

PROGRAM FOR NEXT QUARTER

An appreciable portion of the effort during the second quarter will be directed towards fabrication and evaluation of vacuum tight AL 300, AL 995, BeO and double disc alumina windows.

A second group of BeO blocks will be metalized and brazed into test sections which will be ready for high power testing by November 1, 1962. A sapphire thin disc window test section is complete and will be tested during October. Fabrication of the alumina block assemblies has not yet begun but is tentatively scheduled for completion and test during December, 1962.

All hardware for brazing of a double thin disc AL 300, FC 75 cooled window has now been machined, and brazing should be completed by November 1, 1962, provided the thin disc assembly techniques succeed on the first few tries. The heat exchanger for cooling this window is scheduled for delivery early in October 1962.

The first ceramic coatings of V_2O_3 on block windows are scheduled for completion and power tests by mid quarter.

Broad banding of double disc configurations will continue throughout the next period, as will investigation of the seriousness of the ghost mode problem.

APPENDIX

A. DERIVATION OF GHOST MODE RESONANCES

Staprans and Mercer[4] have rearranged, in perhaps more useful form, the original derivation of Forrer and Jaynes[6] of the ghost mode resonances in a planar geometry. The ghost mode resonances are modes which would normally propagate in the dielectric filled waveguide but are cut off in the guide of unity dielectric.

Figure A-1 illustrates a transverse dielectric slab window, the dimensions of which are to be found in order that the window be mode free over a given band of frequencies about the center frequency at which the window is resonant.

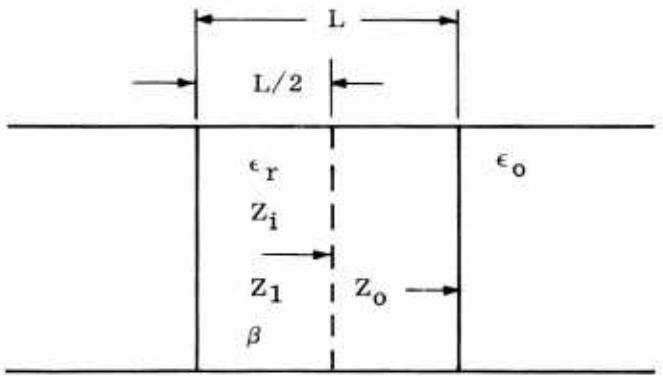

FIGURE A-1
TRANSVERSE TO WAVEGUIDE DIELECTRIC BLOCK WINDOW

By inspection of Forrer and Jaynes' Figure 3, it is seen that computation of first order odd modes or higher is not necessary if operation is nominally close to waveguide cutoff or $(k_c)_{m,n}L < 1.2$. Using the nomenclature from this figure, it can be shown from transmission line equations that:

$$Z_i = Z_1 \frac{\left[Z_o \cos\frac{\beta L}{2} + jZ_1 \sin\frac{\beta L}{2} \right]}{\left[Z_1 \cos\frac{\beta L}{2} + jZ_o \sin\frac{\beta L}{2} \right]} \qquad (1)$$

For example see Ramo and Whinnery,[5] from which it can also be found that for TE and TM waves in a guide the wave impedances are respectively:

$$Z_{TE} = \sqrt{\frac{\mu}{\epsilon}} \left[1 - \left(\frac{f_c}{f}\right)^2\right]^{-1/2} \tag{2}$$

and

$$Z_{TM} = \sqrt{\frac{\mu}{\epsilon}} \left[1 - \left(\frac{f_c}{f}\right)^2\right]^{1/2} \tag{3}$$

For both TE and TM waves:

$$\beta = \frac{\omega}{v} \left[1 - \left(\frac{f_{c_1}}{f}\right)^2\right]^{1/2}, \quad f > f_c \tag{4}$$

Modes which are cut off in the air filled waveguide ($\epsilon = \epsilon_o$, $f < f_c$) but not in the ceramic filled waveguide ($\epsilon = \epsilon_r \epsilon_o$, $f > f_{c_1}$) will result in resonances or ghost modes at certain frequencies. In the case of TM waves, $Z_i \rightarrow 0$ at resonance so the numerator of (1) vanishes; in the case of TE waves $Z_i \rightarrow \infty$ at resonance so the denominator of (1) vanishes. Substitution of (4) and (2) or (3) into (1) results in a transcendental equation (one for each case) which has as solutions the ghost mode frequencies.

For either TE or TM waves

$$f_c = \frac{k_c}{2\pi\sqrt{\mu\epsilon}} = \frac{Ck_c}{2\pi\sqrt{\epsilon_r}} = \frac{1}{\sqrt{\epsilon_r}} \frac{Ck_c}{2\pi} \tag{5}$$

where

C = speed of light

from which it follows that

$$f_{c_1} = \frac{1}{\sqrt{\epsilon_r}} f_c \tag{6}$$

Solutions of interest are those for which

$$\frac{1}{\sqrt{\epsilon_r}} f_c < f < f_c$$

For TM Modes: When the numerator vanishes

$$Z_o \cos \frac{\beta L}{2} + jZ_1 \sin \frac{\beta L}{2} = 0$$

$$\tan \frac{\beta L}{2} = \frac{+jZ_o}{Z_1} \tag{7}$$

from Equation (3)

$$jZ_o = j\sqrt{\frac{\mu_o}{\epsilon_o}} \left[1 - \left(\frac{f_c}{f}\right)^2\right]^{1/2}$$

$$= \sqrt{\frac{\mu_o}{\epsilon_o}} \left[\left(\frac{f_c}{f}\right)^2 - 1\right]^{1/2} \tag{8}$$

from Equation (3)

$$Z_1 = \sqrt{\frac{\mu_o}{\epsilon_r \epsilon_o}} \left[1 - \frac{1}{\epsilon_r}\left(\frac{f_c}{f}\right)^2\right]^{1/2} \tag{9}$$

from Equation (4)

$$\frac{\beta L}{2} = 2\pi f \sqrt{\mu_o \epsilon_o \epsilon_r} \left[1 - \frac{1}{\epsilon_r}\left(\frac{f_c}{f}\right)^2\right]^{1/2} \frac{L}{2}$$

$$= \frac{\pi f_c L}{C} \left[\epsilon_r \left(\frac{f}{f_c}\right)^2 - 1\right]^{1/2}$$

$$= \left(\frac{Ck_c}{2\pi f_c}\right) \frac{\pi f_c L}{C} \left[\epsilon_r \left(\frac{f}{f_c}\right)^2 - 1\right]^{1/2}$$

$$\frac{\beta L}{2} = \frac{k_c L}{2} \left[\epsilon_r \left(\frac{f}{f_c}\right)^2 - 1\right]^{1/2} \tag{10}$$

Combining Equations (10), (8) and (9) with Equation (7) gives

$$\tan \frac{k_c \ell}{2} \left[\epsilon_r \left(\frac{f}{f_c} \right)^2 - 1 \right]^{1/2} = \sqrt{\epsilon_r} \left[\frac{\left(\frac{f_c}{f} \right)^2 - 1}{1 - \frac{1}{\epsilon_r} \left(\frac{f_c}{f} \right)^2} \right]^{1/2} \tag{11}$$

For TE Modes: When the denominator vanishes

$$Z_1 \cos \frac{\beta \ell}{2} + jZ_o \sin \frac{\beta L}{2} = 0$$

$$\cot \frac{\beta \ell}{2} = \frac{-jZ_o}{Z_1} \tag{12}$$

from Equation (2)

$$-jZ_o = -j \sqrt{\frac{\mu_o}{\epsilon_o}} \left[1 - \left(\frac{f_c}{f} \right)^2 \right]^{-1/2}$$

$$-jZ_o = \sqrt{\frac{\mu_o}{\epsilon_o}} \left[\left(\frac{f_c}{f} \right)^2 - 1 \right]^{-1/2} \tag{13}$$

from Equation (2)

$$Z_1 = \sqrt{\frac{\mu_o}{\epsilon_r \epsilon_o}} \left[1 - \frac{1}{\epsilon_r} \left(\frac{f_c}{f} \right)^2 \right]^{-1/2} \tag{14}$$

Combining Equations (10), (14) and (13) with Equation (12) gives

$$\cot \frac{k_c \ell}{2} \left[\epsilon_r \left(\frac{f}{f_c} \right)^2 - 1 \right]^{1/2} = \sqrt{\epsilon_r} \left[\frac{1 - \frac{1}{\epsilon_r} \left(\frac{f_c}{f} \right)^2}{\left(\frac{f_c}{f} \right)^2 - 1} \right]^{1/2} \tag{15}$$

Solutions of (11) and (15) give the even ghost mode solutions corresponding to equations (6b) and (8a) of Forrer and Jaynes.[6] For a given ϵ_r and (f_c/f), the equations are readily solved for $k_c L$.

Up to this point, the mode subscripts have not been used but will now be introduced. Thus $(k_c)_{m,n}$ is the wave number of the mode which propagates with m variations in the width dimension (a) and n variations in the heighth dimension (b). From Ramo and Whinnery,

$$\left(k_c\right)_{m,n} = \frac{\pi}{a}\sqrt{m^2 + n^2\left(\frac{a}{b}\right)^2} \tag{16}$$

$$\left(f_c\right)_{m,n} = \frac{\left(k_c\right)_{m,n}}{2\pi\sqrt{\mu_o \epsilon_o \epsilon_r}} \tag{17}$$

$$\lambda_g = \frac{\lambda}{\sqrt{1 - \left(\frac{f_c}{f}\right)^2}}$$

$$= \frac{C}{f\sqrt{\epsilon_r}\sqrt{1 - \frac{1}{\epsilon_r}\left(\frac{f_c}{f}\right)^2}}$$

$$\lambda_g = \frac{\lambda_o}{\sqrt{\epsilon_r - \left(\frac{\lambda_o}{\lambda_c}\right)^2}} \tag{18}$$

In order to find the length of the window for a given center frequency f_o, set L equal to $\frac{\lambda g}{2}$ where λ_g is measured in the ceramic filled guide. Since the fundamental mode is used in the guide, $(\lambda_c)_{TE_{10}^{\square}} = 2a$ is used.

$$L = \frac{\lambda_g}{2} = \frac{\lambda_o}{2\sqrt{\epsilon_r - \left(\frac{\lambda_o}{2a}\right)^2}} \tag{19}$$

Since λ_o is the free space wavelength corresponding to f_o, L and a are uniquely related.

$$\left(k_c\right)_{m,n} L = \frac{\left(k_c\right)_{m,n}}{\left(k_c\right)_{1,0}} \left(k_c\right)_{1,0} L = \left(k_c\right)_{1,0} L \sqrt{m^2 + n^2\left(\frac{a}{b}\right)^2} \tag{20}$$

$$\left(k_c\right)_{m,n} L = \sqrt{m^2 + n^2\left(\frac{a}{b}\right)^2}\left(\frac{\pi}{a} L\right) \tag{21}$$

$$\left(k_c\right)_{m,n} L = \sqrt{m^2 + n^2\left(\frac{a}{b}\right)^2} \; \frac{\pi\left(\frac{\lambda_o}{\lambda_c}\right)}{\sqrt{\epsilon_r - \left(\frac{\lambda_o}{\lambda_c}\right)^2}} \tag{21a}$$

The relationships to be solved are as follows:

$$L = \frac{\lambda_g}{2} \text{ ceramic} = \frac{\lambda_o}{2\sqrt{\epsilon_r - \left(\frac{\lambda_o}{2a}\right)^2}} \tag{19}$$

λ_o = free space wavelength corresponding to the frequency f_o.

f_o = center frequency of band

ϵ_r = relative dielectric constant of ceramic

a = width of ceramic-filled waveguide

$$\left(k_c\right)_{m,n} L = \sqrt{m^2 + n^2\left(\frac{a}{b}\right)^2}\left(\frac{\pi L}{a}\right) \tag{21}$$

For TE Modes:

$$\cot\left\{\frac{k_{c_{m,n}} L}{2}\left[\epsilon_r\left(\frac{f}{f_c}\right)^2_{m,n} - 1\right]^{1/2}\right\} = \sqrt{\epsilon_r}\left[\frac{1 - \frac{1}{\epsilon_r}\left(\frac{f_c}{f}\right)^2_{m,n}}{\left(\frac{f_c}{f}\right)^2_{m,n} - 1}\right]^{1/2} \tag{15}$$

For TM Modes:

$$\tan\left\{\frac{k_{c_{m,n}} L}{2}\left[\epsilon_r\left(\frac{f}{f_c}\right)^2_{m,n} - 1\right]^{1/2}\right\} = \sqrt{\epsilon_r}\left[\frac{\left(\frac{f_c}{f}\right)^2_{m,n} - 1}{1 - \frac{1}{\epsilon_r}\left(\frac{f_c}{f}\right)^2_{m,n}}\right]^{1/2} \tag{11}$$

where (11) and (15) are to be solved for frequencies such that

$$\frac{1}{\sqrt{\epsilon_r}} f_c < f < f_c$$

f = resonant frequency corresponding to the ghost mode having an air-filled waveguide cutoff frequency $(f_c)_{m,n}$ and wave number $(k_c)_{m,n}$.

Assuming an ϵ_r, equations (11) and (15) can readily be solved for $(k_c)_{m,n}L$ as a function of $(f_c/f)_{m,n}$. Assuming ϵ_r and an a (or b by combining 19 and 21), $(k_c)_{m,n}L$ can be solved for as a function of a/b. Thus $(f_c/f)_{m,n}$ and so $f_{m,n}$ can be found in terms of a/b for each mode.

First Order Even TE Modes:

$$\cot A = B$$

First Order Even TM Modes:

$$\tan A = \epsilon_r \frac{1}{B}$$

$$\cot A = \frac{B}{\epsilon_r}$$

$$A = \left[m^2 + n^2 \left(\frac{a}{b}\right)^2\right]^{1/2} \left[\epsilon_r \left(\frac{f}{f_c}\right)^2_{m,n} - 1\right]^{1/2} \frac{\pi\left(\frac{\lambda_o}{2a}\right)}{2\sqrt{\epsilon_r - \left(\frac{\lambda_o}{2a}\right)^2}}$$

$$B = \sqrt{\epsilon_r}\left[\frac{1 - \frac{1}{\epsilon_r}\left(\frac{f_c}{f}\right)^2_{m,n}}{\left(\frac{f_c}{f}\right)^2_{m,n} - 1}\right]^{1/2}$$

B. HEAD LOSS IN DUAL DISC WINDOW COOLING

The cross sectional view of the proposed 1.4 inch diameter double disc window is shown in Figure A-2.

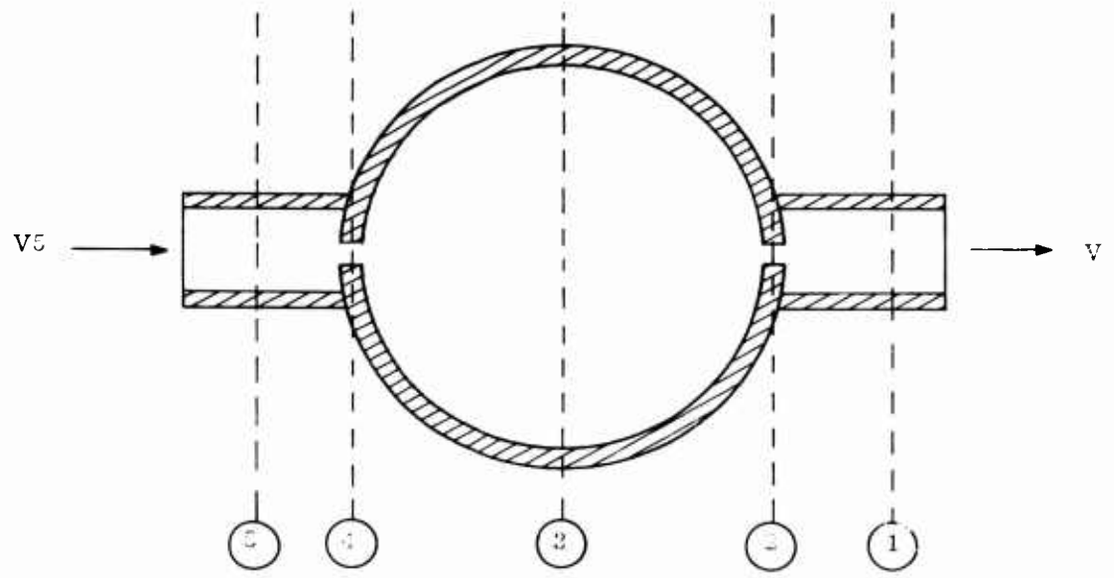

FIGURE A-2
CROSS SECTION OF PROPOSED DOUBLE DISC FLUID COOLED WINDOW

It is seen that due to the necessity of keeping the vents to the volume between the discs small (short length and restricted width) there are four sudden constrictions and enlargements. Each one of these will be responsible for a certain amount of head or pressure loss. It is the purpose here to approximate these losses and to determine optimum flow conditions.

It is assumed in the beginning that the pressure and velocity in area 1 are zero or equivalent to the flow dumping into a resevoir. Using a form of the equation of continuity

$$A_1V_1 = A_2V_2 = Q$$

where

A = cross sectional area of flow

V = velocity (ft/sec)

Q = flow rate (ft^3/sec)

the velocity at any point in the system can be calculated for a given flow rate. Assuming

$$Q = .5 \text{ gal/minute } (2.23 \times 10^{2} ft^3/sec)$$

and

$$A_2 = 3.333 \times 10^{-5} ft^2$$

(from .12 x .04 inch slot)

$$V_2 = 33.5 \text{ ft/sec}$$

The head loss in going from point 3 to point 2 (a sudden constriction) can be approximated by the use of

$$h_L = K_L \frac{V_2^2}{2g}$$

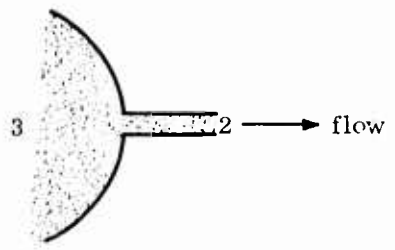

Vennard[7] gives a value for $K_L = 0.46$ when the ratio of $\frac{A_2}{A_3}$ equals 0.174

$$(A_3 = 1.32 \times 0.04 \text{ in}^2)$$

Therefore $h_{L\ 32} = 8.03$ ft or $P_{Lost\ 32} = \gamma h_{L\ 32} = 6.16$ psi. γ = specific weight of FC 75 = 110.5 lb/ft^3.

A solution of Bernoullis equation

$$\frac{P_3}{\gamma} + \frac{V_3^2}{2g} = \frac{P_2}{\gamma} + \frac{V_2^2}{2g} + h_{L\ 32}$$

for P_3 gives a value of $P_3 = 20$ psi.

Note that the pressure at point 2 is taken to be 78.05 lb/ft^2 which is as low as it can be and still result in non-cavitatious flow. It is determined as the vapor pressure of FC 75 at whatever the operating temperature is. In this case 25°C was assumed.

On entering point 3 from point 4 (Figure A-2) another head loss is encountered but this time through an enlargement in the flow path.

$$\text{Using } k_{L\,43} = K_L \frac{(V_4 - V_3)^2}{2g} \text{ where } K_L \simeq 1 \text{ and } V_4 = V_2 \text{ from continuity}$$

$$h_{L\,43} = 14.43 \text{ ft}$$

$$P_{\text{Lost } 43} = 11.08 \text{ psi}$$

Again using Bernoullis equation including head loss from 4 to 3

$$P_{43} = 18 \text{ psi.}$$

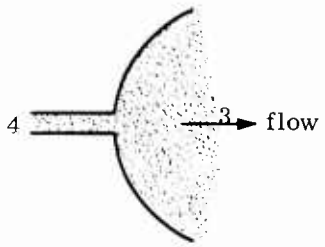

Similar analysis through the remainder of the flow path gives results which are tabulated with the previous ones in Table A-1.

TABLE A-1
TABULATED CALCULATED RESULTS

POINT	VELOCITY FT/SEC	PRESSURE PSI GAGE	TOTAL HEAD LOSS
2	33.5	.54	
3	3.04	20	
4	33.5	18	
5	5.82	36.6	47.23 ft.

One of the requirements for coolant flow is that it be turbulent--that is, where the fluid experiences a complete mixing of the fluid particles as flow takes place. Reynolds number serves as an excellent indication of whether a particular flow is turbulent.

$$N_R = \frac{VdP}{u}$$

where

V = velocity in feet per sec

d = diameter of flow path in feet

P = density in slugs per cubic foot

μ = viscosity in pound-seconds per square foot

The upper critical Reynolds number at which laminar flow ceases is normally 4000 in practical engineering problems. A solution of the above equation for the region between the window discs (region 3) yields a number of 9350. This is assuming an average flow diameter of 0.0156 foot and

where

$$P = 3.425$$

$$\mu = 2.405 \times 10^{-5}$$

Thus, a flow of 0.5 gallon per minute of FC 75 will provide adequate turbulent flow at a pressure of about 20 psi. Additional improvement can be made in the flow path to reduce flow losses by tapering the abrupt constrictions as much as possible.

DISTRIBUTION LIST

Copy No.	No. of Copies	Address
1 - 8	8	**RADC (RALTP, ATTN: D. Bussey) Griffiss AFB NY
9	1	*RADC (RAAPT) Griffiss AFB NY
10	1	*RADC (RAALD) Griffiss AFB NY
11	1	*GEEIA (ROZMCAT) Griffiss ABF NY
12	1	*RADC (RAIS, ATTN: Mr. Malloy) Griffiss AFB NY
13	1	*Signal Corps Liaison Officer RADC(RAOL, ATTN: Maj Norton) Griffiss AFB NY
14	1	*AUL (3T) Maxwell AFB Ala
15	1	ASD (ASAPRD) Wright-Patterson AFB Ohio
16	1	Chief, Naval Research Lab ATTN: Code 2027 Wash 25 DC
17	1	Air Force Field Representative Naval Research Lab ATTN: Code 1010 Wash 25 DC
18	1	Commanding Officer USASRDL ATTN: SIGRA/SL-ADT Ft Monmouth NJ
19	1	National Aeronautics and Space Admin Langley Research Center Langley Station Hampton Virginia ATTN: Librarian
20	1	Central Intelligence Agency ATTN: OCR Mail Room 2430 E Street NW Wash 25 DC
21	1	US Strike Command ATTN: STRJ5-OR Mac Dill AFB Fla
22	1	AFSC (SCSE) Andrews AFB Wash 25 DC
23	1	Commanding General US Army Electronic Proving Ground ATTN: Technical Documents Library Ft Huachuca Ariz
24 - 33	10	*ASTIA (TISIA-2) Arlington Hall Station Arlington 12 Va
34	1	AFSC (SCFRE) Andrews AFB Wash 25 DC
35	1	Hq USAF (AFCOA) Wash 25 DC
36	1	AFOSR (SRAS/Dr. G. R. Eber) Holloman AFB NMex
37	1	Office of Chief of Naval Operations (Op-724) Navy Dept Wash 25 DC
38	1	Commander US Naval Air Dev Cen (NADC Lib) Johnsville Pa
39	1	Commander Naval Missile Center Tech Library (Code NO 3022) Pt Mugu Calif
40	1	Bureau of Naval Weapons Main Navy Bldg Wash 25 DC ATTN: Technical Librarian, DL1-3
41	1	Redstone Scientific Information Center US Army Missile Command Redstone Arsenal, Alabama
42	1	Commandant Armed Forces Staff College (Library) Norfolk 11 VA
43	1	ADC (ADOAC-DL) Ent AFB Colo
44	1	AFFTC (FTOOT) Edwards AFB Calif
45	1	Commander US Naval Ordnance Lab (Tech Lib) White Oak, Silver Springs Md
46	1	Commanding General White Sands Missile Range New Mexico ATTN: Technical Library
47	1	Director US Army Engineer R and D Labs Technical Documents Center Ft Belvoir VA
48	1	ESD (ESRL) L G Hanscom Fld Bedford Mass
49	1	Commanding Officer and Director US Navy Electronics Lab (LIB) San Diego 52 Calif
50	1	ESD (ESAT) L G Hanscom Fld Bedford Mass
51	1	Commandant US Army War College (Library) Carlisle Barracks Pa
52	1	APGC (PGAPI) Eglin AFB Fla
53	1	AFSWC (SWOI) Kirtland AFB NMex
54	1	AFMTC (Tech Library MU-135) Patrick AFB Fla
55	1	European GEEIA Rgn (ZEM) APO 332 New York NY
56	1	Hq Pacific GEEIA Rgn (ZPM) APO 915 San Francisco Calif
57	1	Western GEEIA Rgn (ZSM) McClellan AFB Calif
58	1	Eastern GEEIA Rgn (ZMMRS) Brookley AFB Ala
59	1	Inspection Office (Tech Lib) Central GEEIA Rgn (AFLC) Tinker AFB Okla
60	1	Dr. Louis R. Bloom Sylvania Elect Prod Inc. Physics Lab 208-20 Willetts Point Blvd Bayside, Long Island, N.Y.

*Mandatory

**Project Engineer will enter his symbol and name in the space provided.

DISTRIBTUION LIST (Cont.)

Copy No.	No. of Copies	Address
61 - 62	2	Technical Library Varian Associates 611 Hansen Way Palo Alto, California
63	1	Dr. L. A. Roberts Watkins Johnson Co Palo Alto, California
64	1	Mr. Gerald Klein, Mgr Microwave Tube Section Applied Research Dept Westinghouse Elect Corp Friendship Intl Airport Box 746 Baltimore, Md.
65	1	Hughes Aircraft Co Culver City, Calif ATTN: Everett M. Wallace
66	1	Bendix Aviation Corp Red Bank Division Eatontown, New Jersey ATTN: John Johnstone
67 - 68	2	Eitel Mc Cullough Inc 901 Industrial Way San Carlos, California ATTN: Stella R. Vetter Research Library
69	1	Mr. F. E. Ferrira Director of Research Coors Porcelain Co Golden, Colorado
70 - 71	2	Mr. M. Hoover RCA Lancaster, Pa
72	1	Dr. D. Goodman Sylvania Microwave Tube Lab 500 Evelyn Avenue Mt. View, California
73	1	Mr. A. E. Harrison University of Washington Dept of Elect Engineering Seattle 5, Washington
74	1	Mr. Shelden S. King Eng Librarian Westinghouse Elect Corp PO Box 284 Elmira, New York
75	1	Kane Engineering Labs 460 Cambridge Avenue Palo Alto, California ATTN: Mr. F. Kane
76	1	Electrical Industries Co Murray Hill, New Jersey ATTN: Mr. Peter A. Muto
77	1	Mr. L. E. Gates, Jr. 20/1365 41-48-20 Hughes Aircraft Co Culver City, California
78	1	Mr. Theodore Poumbanis Microwave Elect Prod Inc Microwave Device Operations 600 Evelyn Avenue Mountain View, California
79	1	Dr. R. G. E. Hutter Sylvania Microwave Tube Lab 500 Evelyn Ave Mt. View, California
80	1	Dr. William Watson Litton Industries 960 Industrial Road San Carlos, Calif
81	1	Technical Library Litton Industries 960 Industrial Road San Carlos, Calif
82	1	Mr. Ted Moreno Varian Associates 611 Hansen Way Palo Alto, Calif
83	1	Mr. C. Dalman Cornell University Dept of Elect Eng Ithaca, New York
84	1	Mr. Donald Priest Eitel-Mc Cullough Inc San Bruno, California
85	1	Mr. T. Marchese Federal Tele Labs Inc 500 Washington Ave Nutley, New Jersey
86	1	Mr. S. Webber General Elect Microwave Lab 601 California Ave Palo Alto, California
87	1	Dr. Harold Sobol IBM Research Laboratory Bldg 701 Room W 164 Poughkeepsie, New York
88	1	Dr. D. D. King Johns Hopkins University Radiation Laboratory Baltimore 2, Maryland
89	1	Mr. R. Butman M.I.T. Lincoln Laboratory PO Box 73 Lexington 73, Mass.
90	1	Dr. S. F. Kaisel Microwave Electronics Corp 4061 Transport Street Palo Alto, California
91	1	Ohio State University Dept of Elect Engineering Columbus 10, Ohio ATTN: Prof. E. M. Boone
92	1	Mr. W. C. Brown Spencer Lab Raytheon Mfg Co Wayside Rd Burlington, Mass.
93	1	Mr. W. Teich Raytheon Mfg Co Spencer Lab Burlington, Mass.
94	1	Mr. Hans Jenny RCA Elect Tube Div 415 South 5th Street Harrison, New Jersey
95	1	Mr. P. Bergman Sperry Corp Elect Tube Div Gainesville, Florida
96	1	Dr. M. Chodorow Stanford University Microwave Lab Stanford, California
97	1	Dr. Bernard Arfin Varian Associates 611 Hansen Way Palo Alto, California
98	1	Dept of Electrical Eng University of Florida Gainsville, Florida
99	1	Dr. E. D. Mc Arthur General Elect Co Electron Tube Div of Research Lab The Knolls Schenectady, New York
100	1	Mr. J. T. Milek Hughes Aircraft Co Electron Tube Laboratory Culver City, California
101	1	University of Illinois Electrical Eng Research Lab Urbana, Ill ATTN: Technical Editor

DISTRIBUTION LIST (Cont.)

Copy No.	No. of Copies	Address
102	1	Dr. Norman Moore Litton Industries 960 Industrial Road San Carlos, California
103	1	Mass Institute of Technology Research Laboratory of Electronics Cambridge 39, Mass. ATTN: Document Library
104	1	University of Minnesota Minneapolis, Minnesota ATTN: Dr. W. G. Shepherd Dept of Elect Eng
105	1	Dr. M. Ettinberg, Polytechnic Institute of Brooklyn Microwave Research Inst Brooklyn 1, New York
106	1	Mr. John M. Osepchuk Raytheon Co Spencer Lab Burlington, Mass
107	1	Dr. Bernard Hershenon RCA Labs Princeton, New Jersey
108	1	Dr. W. M. Webster Director Electronic Research Lab RCA Labs Princeton, New Jersey
109	1	Stanford University Elect Research Laboratory Stanford, California ATTN: Mr. D. C. Bacon Asst Director
110	1	Dr. D. A. Watkins Stanford University Electronics Laboratory Stanford, California
111	1	Secretariat Advisory Group on Electron Tubes 346 Broadway New York 13, New York
112	1	Bell Telephone Labs Murry Hill Laboratory Murry Hill, New Jersey ATTN: Dr. J. R. Pierce
113	1	Mr. A. G. Peifer Bendix Corporation Systems Planning Div Ann Arbor, Michigan
114	1	Professor R. M. Saunders University of California Dept of Engineering Berkeley 4, California
115 - 116	2	Commanding Officer US Army Signal R and D Lab ATTN: Logistics Div (SIGRA/SL-PRT) L. N. Heynick Ft. Monmouth New Jersey
117	1	Field Emession Corp. 611 Third Street McMinnville Oregon ATTN: Mr. F. M. Charbonnier
118	1	Dr. Robert T. Young Chief Electron Tube Branch Diamond Ord Fuse Lab Washington 25, D.C.
119	1	Applied Radiation Co Walnut Creek California ATTN: Mr. Niel J. Norris
120	1	Dr. J. H. Bryant Bendix Corporation Research Labs Northwestern Hghy and 10 1/2 Mile Road Detroit 35, Michigan
121	1	The Electronics Research Lab 427 Cory Hall The University of California Berkeley 4, California ATTN: Mrs. Simmons
122	1	Professor W. G. Worcester University of Colorado Dept of Electrical Engineering Boulder, Colorado
123	1	Columbia University Columbia Radiation Lab 538 W 120th Street New York 27, N.Y.
124	1	Mr. Lester Firestein Stanford Research Institute Palo Alto California
125 - 150	26	Retained by Varian Associates

UNCLASSIFIED